Elsevier Editorial System(tm) for Acta Biomaterialia
Manuscript Draft

Manuscript Number:

Title: Development of Novel Nanoparticles Shelled with Heparin for Berberine Delivery to Treat Helicobacter pylori

Article Type: Full Length Article

Keywords: Helicobacter pylori; berberine; heparin; nanoparticles; intercellular spaces

Corresponding Author: Dr Yu-Hsin Lin,

Corresponding Author's Institution: China Medical University

First Author: Chiung-Hung Chang

Order of Authors: Chiung-Hung Chang; Shu-Fen Peng; Chih-Ho Lai, ; Yi-Hsing Yao; Ting-Yu Chen; Jing-Yan Wu; Wen-Ying Huang; Tsai-Luan Chang; Ming-Ju Liu; Yu-Hsin Lin

Abstract: A variety of approaches have been studied to overcome problems encountered with using antibiotics, which are ineffective in treating Helicobacter pylori infection and the occurrence of unpleasant side effects. This situation has forced researchers to look for alternative strategies to eliminate H. pylori infection. The plant alkyloid berberine has been shown to significantly reduce proliferation of H. pylori. In order to localize berberine to the H. pylori infection site, we developed a novel nanoparticle berberine carrier shelled with heparin. Analysis revealed that our in vitro drug carrier system is able to control berberine release in the simulated gastrointestinal medium, and that the berberine was able to interact specifically with intercellular space at the site of H. pylori infection. Furthermore, the prepared nanoparticles were able to significantly increase the capacity of berberine to inhibit the growth of H. pylori, while efficiently decreasing the cytotoxic effects within the H. pylori infected cells.

May 15, 2010

Professor W.R. Wagner
Editor-in-Chief, Acta Biomaterialia

Dear Professor Wagner:

Attached please find a manuscript entitled "Development of novel nanoparticles shelled with heparin for berberine delivery to treat *Helicobacter pylori*". The manuscript is intended to be published in *Acta Biomaterialia*. It has been sorely submitted to *Acta Biomaterialia* and that it is not concurrently under consideration for publication in any other journal. We value you and the reviewers' suggestions and comments.

Thank you in advance for arranging the review process for our manuscript. We look forward to hearing from you soon.

Sincerely yours,

Yu-Hsin Lin, PhD
Assistant Professor
Department of Biological Science and Technology
China Medical University,
Taichung, Taiwan, 40402
Fax: 886-4-2207-1507
E-mail: ylhsin@mail.cmu.edu.tw

**Suggested reviewers:**

1. **Prof. C. Perry Chou.** Departments of Chemical Engineering and Biology, Waterloo University, 200 University Avenue West, Waterloo, Ontario, Canada. Email: cpchou@uwaterloo.ca
2. **Prof. Tatsuo Yamamoto.** Infectious Diseases and International Medicine, Niigata University, JP. E-mail: tatsuoy@med.niigata-u.ac.jp
3. **Prof. Fwu-Long Mi.** Department of Biotechnology, Vanung University, Chungli, Taoyuan, Taiwan, ROC. E-mail: flmi530326@mail.vnu.edu.tw

**Development of Novel Nanoparticles Shelled with Heparin for Berberine Delivery to Treat *Helicobacter pylori***

Chiung-Hung Chang[1†], Shu-Fen Peng[2†], Chih-Ho Lai[3], Yi-Hsing Yao[2], Ting-Yu Chen[2], Jing-Yan Wu[2], Wen-Ying Huang[4], Tsai-Luan Chang[4], Ming-Ju Liu[4], Yu-Hsin Lin[2#]

[1] School of Chinese Medicine, China Medical University, Taichung, Taiwan, ROC.
[2] Department of Biological Science and Technology, Center for Inflammation Research, China Medical University, Taichung, Taiwan, ROC.
[3] Department of Microbiology, School of Medicine, China Medical University, Taichung, Taiwan, ROC.
[4] Department of Applied Cosmetology and Graduate Institute of Cosmetic Science Hungkuang University, Taichung, Taiwan, ROC.

#Correspondence to:

Yu-Hsin Lin, PhD
Assistant Professor
Department of Biological Science and Technology
China Medical University,
Taichung, Taiwan, 40402
Fax: 886-4-2207-1507
E-mail: ylhsin@mail.cmu.edu.tw

†The first two authors (Chiung-Hung Chang and Shu-Fen Peng) contributed equally to this work.

**Abstract**

A variety of approaches have been studied to overcome problems encountered with using antibiotics, which are ineffective in treating *Helicobacter pylori* infection and the occurrence of unpleasant side effects. This situation has forced researchers to look for alternative strategies to eliminate *H. pylori* infection. The plant alkyloid berberine has been shown to significantly reduce proliferation of *H. pylori*. In order to localize berberine to the *H. pylori* infection site, we developed a novel nanoparticle berberine carrier shelled with heparin. Analysis revealed that our *in vitro* drug carrier system is able to control berberine release in the simulated gastrointestinal medium, and that the berberine was able to interact specifically with intercellular space at the site of *H. pylori* infection. Furthermore, the prepared nanoparticles were able to significantly increase the capacity of berberine to inhibit the growth of *H. pylori*, while efficiently decreasing the cytotoxic effects within the *H. pylori* infected cells.

Keywords: *Helicobacter pylori*; berberine; heparin; nanoparticles; intercellular spaces

## 1. Introduction

Gastric ulcer disease is a global health concern because of the considerable economic burden associated with its high morbidity and mortality rates [1]. *Helicobacter pylori* infection is considered to be a primary risk factor for development of gastric ulcers and gastric cancer [2]. The bacterium *H. pylori* produces the enzyme urease, which is able to hydrolyze urea to ammonia and bicarbonate in order to neutralize the acidic pH of stomach environment. It has been reported that the normal gastric pH of approximately 1 to 3 can be elevated to about 4.5–7.0, thus creating an environment conducive to *H. pylori* colonization [3]. Moreover, the microorganism mainly exists deep within the gastric mucus layer where it adheres to gastric epithelial cells through a variety of adhesion-like proteins [3,4]. In order to effectively eradicate *H. pylori* infection, the therapeutic agent must be able to penetrate through the gastric mucus layer and maintain a concentration sufficient for antibacterial activity at the infected site for a suitable length of time. The most widely recommended regimen includes a triple therapy which combines various antibiotics (amoxicillin, clarithromycin, and metronidazole) and a proton pump inhibitor administered over a period of two weeks [5]. However, the occurrence of unpleasant side effects, such as a metallic taste in the mouth, diarrhea and nausea, may cause the patient to interrupt the prescribed course of antibiotics, thus promoting the development of bacterial resistance [6]. This situation has forced researchers to look for alternative strategies to treat and eradicate *H. pylori* infection.

Several herbal medicines have been tested for their potential antibacterial activity against *H. pylori in vitro* and in clinical studies as possible candidates for use in modified eradication therapy [2,7]. Berberine (structure shown in Figure 1) is an isoquinoline quaternary alkaloid derived from a number of species of the barberry plant, including *Berberis aristate* and *Coptis chinensis* [8]. Berberine has been used for over 2000 years in traditional Eastern medicine to treat gastro–enteritis and secretory diarrhea and is also effective in prevention and treatment of diarrheal illness [9]. Recent pharmacological studies have demonstrated that berberine is able to exert

inhibitory effects on the proliferation capacity of *H. pylori* and the activity of its *N–acetyltransferase* [10]. Thus, berberine could act to reduce the growth of *H. pylori* in infected individuals, promote anti–neoplastic activity of gastric cancer cells and protect gastric mucosa from damage [11–13]. However, it is unknown whether berberine may be able to readily penetrate the epithelia. Therefore, we sought to develop a site–specific drug delivery system that would facilitate not only penetration of the stomach mucus layer but also deliver a sufficient concentration of berberine to eradicate *H pylori* infection.

In order to localize berberine at the *H. pylori* infection site on the gastric epithelium where it may improve the efficacy of concomitantly administered anti–*H. pylori* agents, a novel nanoparticle shelled with heparin was developed as berberine delivery system. Heparin is a polyanionic mucopolysaccharide with a mean molecular weight (MW) of 15 kDa (approximately 45 monosaccharide chains). The polymeric chain is composed of repeating disaccharide units of D–glucosamine and uronic acid linked by 1→4 interglycosidic bonds. The uronic acid residue can be either D–glucuronic acid or L–iduronic acid [14]. Recently, heparin, a well-known anticoagulant, has been reported to have the ability to bind to cell receptors and accelerate gastric ulcer healing, which is associated with mucosal regeneration, proliferation and angiogenesis [15,16]. We found that heparin crosslinked with berberine appears to have a heterogeneous size distribution with an oval donut shape (Figure 1 and Figure 2). To form a more suitable complex, we employed chitosan, a cationic polysaccharide known to be non–toxic, bioabsorbable and biocompatible [17,18]. Chitosan has also been proven to adhere to and open the tight junctions between epithelial cells and to increase the permeability of epithelial cell monolayers [19]. When blended with heparin, the resulting chitosan-heparin complex was determined to be spherical in shape with a relatively homogeneous size distribution (Figure 1).

In this study, we prepared nanoparticles composed of berberine, heparin and chitosan in various weight ratios and examined their physicochemical characteristics

with fourier transformed infrared spectroscopy (FT–IR), transmission electron microscopy (TEM), and dynamic light scattering. We also investigated the *in vitro* release characteristics of berberine from the prepared nanoparticles and examine the *in vitro* growth inhibition in *H. pylor* isolates. In addition, the effect of the nanoparticles and their mechanism of interaction were investigated in the human gastric mucosal AGS cell line (human gastric adenocarcinoma cell line) [20] with confocal laser scanning microscopy (CLSM).

## 2. Experiments and protocols

### *2.1. Materials*

Chitosan (MW 50 kDa) with approximately 85% deacetylation was obtained from Koyo Chemical Co. Ltd. (Japan). Heparin (5000 IU/mL, MW 15 kDa, 179 IU/mg) was purchased from Leo Chemical Factory (Ballerup, Denmark). Acetic acid, berberine, phosphate-buffered saline (PBS), 4´,6-diamidino-2-phenylindole (DAPI), fluoresceinamine isomer I (FA), paraformaldehyde, 3-(4,5-dimethyl-thiazol-yl)-2,5-diphenyltetrazolium bromide (MTT), and Hanks' balanced salt solution (HBSS) were purchased from Sigma-Aldrich (St Louis, MO). RPMI 1640, fetal bovine serum (FBS), penicillin, streptomycin, and trypsin–EDTA were from Gibco (Grand Island, NY). 3-(4,5-dimethylthiazol-2-yl)-5-(3-carboxymethoxyphenyl)-2-(4-sulfophenyl)-2H-tetra zolium) (MTS) was purchased from Promega, Madison (WI, USA). DilC18(5)–DS lipophilic dye were purchased from Molecular Probes (Eugene, OR, USA). All other chemicals and reagents were of analytical grade.

### *2.2. Preparation of berberine/heparin/chitosan nanoparticles*

The different composition of nanoparticles (berberine/heparin nanoparticles or berberine/heparin/chitosan nanoparticles) was prepared by a simple ionic gelation method with magnetic stirring at room temperature. Table 1–3 lists the conditions for the nanoparticles preparation, as well as the measured size distribution and zeta

potential values for each test sample. First, the berberine/heparin nanoparticles (Table 1) were prepared by aqueous berberine (0.0375% by w/v) was added by flush mixing with a pipette tip into aqueous heparin at various concentrations (0.0083%, 0.0167%, 0.0333%, 0.0500%, 0.0667% by w/v). Second, the berberine/heparin/chitosan nanoparticles (Table 2–3) at distinct compositions (berberine:heparin:chitosan = 0.0375%:0.0500%:0.0200%, 0.0375%:0.0500%:0.0400%, 0.0375%:0.0500%:0.0800%, 0.0200%:0.0500%:0.0400%, 0.0250%:0.0500%:0.0400%, and 0.0300%:0.0500%:0.0400% by w/v) were prepared by dropping aqueous berberine/heparin solution (0.5 mL) into a aqueous chitosan solution (pH 6.0, 0.5 mL).

*2.3. Characterization of the prepared nanoparticles*

The size distribution and zeta potential of the prepared nanoparticles at DI water were measured using a dynamic light scattering analyzer (Zetasizer ZS90, Malvern Instruments Ltd., Worcestershire, UK). FT–IR spectra of the prepared nanoparticles were recorded with a Fourier transformed infrared spectroscopy (FT–IR, Shimadzu Scientific Instruments, USA). TEM was employed to examine the morphology of the different composition of nanoparticles (berberine/heparin nanoparticles or berberine/heparin/chitosan nanoparticles). The nanoparticle suspension was placed onto a 400 mesh copper grid coated with carbon. About 2 min after deposition, the grid was tapped with a filter paper to remove surface water and positively stained with an alkaline bismuth solution [21].

*2.4. Release profiles of berberine*

To measurement the berberine loading efficiency of the prepared nanoparticles, the resulting solution containing berberine–loaded nanoparticles was centrifuged at 32,000rpm, 4℃ for 50 min. The amount of free berberine concentration in the supernatant was analyzed using a high–performance liquid chromatography (HPLC) [22]. The berberine loading efficiency of the nanoparticles was calculated from the

following equation: [23]

$$\text{Loading efficiency} = \frac{\text{total amount of berberine} - \text{free berberine}}{\text{total amount of berberine}} \times 100\%$$

The release profiles of berberine from test nanoparticles were investigated in simulated dissolution medium (pH 1.2 for 120 min, pH 6.0 for 120 min, then pH 7.0 for 240 min, simulating gastric acid, gastric mucosa and the *H. pylori* survival situation), respectively ($n$ = 5) at 37 °C. At set time intervals, samples were removed and centrifuged, and the supernatants were subjected to HPLC. The percentage of cumulative amount of released berberine was determined by a standard calibration curve. The stability of berberine was determined by analyzing the conformation of the released berberine from nanoparticles using an electrospray ionization–mass spectrometer (ESI–MS) and comparing the spectrum with that of standard berberine. For ESI–MS measurement, berberine released from nanoparticles and standard berberine were separately dissolved at alcohol at the concentrations of 10 ppm directly injected into the electrospray ionization interface of the mass spectrometry. The ionization was on a positive mode with a spray voltage of +4.25 kV [24].

*2.5. In Vitro growth inhibition study*

*H. pylori* strain 26695 (ATCC 700392) was obtained from the American Type Culture Collection (ATCC, Manassas, VA, USA). The bacteria were grown on blood agar plates under microaerophilic conditions for 48–72 hr at 37°C. The colonies were collected and pooled in HBSS solution (pH 6.0) to an optical density of 1.0 at 590 nm ($OD_{590}$), which corresponded to $10^6$ colony–forming units (CFU)/mL bacteria at 590 nm in a visible spectrophotometer (*Biochrom* Ltd., England). To characterize the ability of berberine and berberine–loaded nanoparticles to inhibit growth of *H. pylori*, bacterial suspensions were exposed to berberine solution and berberine/heparin/chitosan nanoparticles with distinct berberine concentrations (0.0, 3.0, 6.0, and 12.0 by mg/L) for 24 hr. Specifically, 5 mL of HBSS solution was inoculated with an equal volume of stock culture; a micropipette was used to aliquot

appropriate volumes of different formulations to culture vials containing the *H. pylori* strain. All mixtures were incubated in a candle jar under microaerophilic conditions with humidity at 37°C. The extent of growth inhibition was determined by $OD_{590}$ measurements at distinct time intervals. Quantification of *in vitro* antibacterial activity was carried out by calculating percentage growth inhibition as compared to untreated *H. pylori*. The percent growth inhibition was determined using the formula [25]:

$$\% \text{ growth inhibition} = \frac{\text{OD of control} - \text{OD of sample}}{\text{OD of control}} \times 100\%$$

where control refers to *H. pylori* broth and sample refers to *H. pylori* broth incubated with formulations.

### *2.6. Viability of AGS cells treated with berberine solution and berberine/heparin/chitosna nanoparticles*

The AGS cell line (ATCC CRL 1739) was obtained from the American Type Culture Collection (ATCC) and used between passages 40 and 60. The cells were initially grown in 25 $cm^2$ tissue culture flasks with RPMI 1640 medium containing 10% FBS, penicillin (100 U/mL), and streptomycin (100 μg/mL) and were kept in an incubator at 37 °C, 95% humidity, and 5% $CO_2$ [3]. The cells were harvested for subculture every three days with 0.25% trypsin plus 0.05% EDTA solution and were used for the cytotoxicity experiments. The cytotoxicity of the test samples was evaluated *in vitro* with the MTT assay. The assay is based on mitochondrial dehydrogenase activity as an indicator of cell viability. Briefly, MTT was dissolved in PBS to a concentration of 5 mg/mL as a stock MTT solution and filtered for sterilization. AGS cells were seeded at $5 \times 10^4$ cells/well in 96-well plates and allowed to adhere overnight. The growth medium was replaced with HBSS solution (pH 6.0) that contained various berberine concentrations (0.0, 3.0, 6.0, and 12.0 by mg/L) of berberine solution and berberine/heparin/chitosna nanoparticles formulation for 2 hr. After 2 hr, the test samples were aspirated and the cells were washed twice with 100 μL of PBS. The cells were then incubated in growth medium for an

additional 22 hr. After specific times, the cells were then incubated in growth medium containing 1 mg/mL MTT for an additional 4 h. Dimethyl sulfoxide (DMSO; 100 μL) was added to each well to ensure the solubilization of the formazan crystals formed. The optical density was read with a Molecular Devices SpectraMax M2$^{e}$ microplate spectrofluorometer (Sunnyvale, CA) at a wavelength of 570 nm. All experiments were performed six times with eight replicate wells for every sample and control per assay.

*2.7. Association of fluorescent H. pylori and nanoparticles with AGS cells and CLSM visualization*

To observe the adhesion of *H. pylori* to cells, the bacterium was labeled with DilC18(5)-DS fluorescently labeled lipophilic dye to form the DilC18(5)–*H. pylori*. The bacteria were collected from the agar plates and resuspended in PBS to an optical density at 590 nm ($OD_{590}$) of 1.0. After centrifugation at 3000 rpm for 10 min, the bacterial pellet was resuspended in 1.0 mL of diluent A. Then 1.0 mL of diluent A containing 50 μL of DilC18(5)–DS dye was added and mixed with the bacterial suspension. The bacterial suspension was mixed again for 5 min at 30°C followed by 15 min incubation on ice. The bacterial pellet was washed three times with ice cold PBS, suspended in PBS, and used to infect cells at a multiplicity of infection (MOI) of 50.

The fluorescent nanoparticles (berberine/FA–heparin/chitosan) were prepared. The synthesis of FA–heparin was based on the reaction between the amine groups of FA and the carboxylic acid groups of heparin [3]. Heparin (3.07 g) and FA (0.0583 g) were dissolved completely in 30 mL of acetonitrile with 0.0408 g of 1-ethyl-3-(3-dimethylaminopropyl)-carbodiimide hydrochloride, and incubated at room temperature for 2 hr. To remove the unconjugated FA, FA–heparin were dialyzed in the dark against 5 L of distilled water, which was replaced on a daily basis until no fluorescence was detected in the supernatant. The resultant FA–heparin was lyophilized in a freeze dryer. The fluorescent nanoparticles were prepared according to the procedure described in preparation of berberine/heparin/chitosan nanoparticles

section.

To track the internalization of the test samples, the cells were seeded onto glass coverslips at a density $3 \times 10^5$ cells/cm$^2$ and incubated for two days. The test samples (DilC18(5)–*H. pylori* and berberine/FA–heparin/chitosan nanoparticles) were then added to the cells for 2 hr. After incubation, the test samples were aspirated. The cells were then washed three times with PBS before they were fixed in 3.7% paraformaldehyde. The cells were examined with excitation at 340 (for berberine), 488 (for FA–heparin), and 633 (for DilC18(5)–*H. pylori*) under a CLSM [26]. The images were superimposed with the LCS Lite software (version 2.0).

*2.8. Evaluating the relationship between H. pylori and nanoparticles*

AGS cells were grown to subconfluence and treated with various berberine concentrations (0.0, 3.0, and 6.0 by mg/L) of berberine/heparin/chitosan nanoparticle formulation for 2 hr. The test samples were then aspirated and the cells were washed twice with PBS and then inoculated with *H. pylori* at a final concentration of $8 \times 10^8$ CFU/mL. After co–culture with *H. pylori* for 2 hr, the treated AGS cells were washed and incubated in growth medium for an additional 22 hr. The amount of growth inhibition on AGS cells by *H. pylori* was analyzed using the trypan blue exclusion [27].

The *in situ* adherence properties of *H. pylori* are useful for identifying effective nanoparticles. The adherence detection protocol used was carried out as previously described, but with the following modifications [25,28]. The constant berberine 6.0 mg/L of berberine/FA–heparine/chitosan nanoparticles diluted in HBSS solution were added directly to the AGS cells for 2 hr. Meanwhile *H. pylori* in log phase was inoculated onto glass coverslips; the AGS treated cells were then added to the labeled DilC18(5)–*H. pylori* at an MOI of 50 and incubated at 37°C for 2 hr. The cells were then washed three times with PBS and fixed in 3.7% paraformaldehyde. Cells were examined by excitation at 340 nm (for berberine), 488 nm (for FA–heparin) and 633 nm (for DilC18(5)–*H. pylori*) under a CLSM. The images were superimposed by the

LCS Lite software (version 2.0).

*2.9. Statistical analysis*

Statistical analysis of the differences in the measured properties of the groups was performed with one-way analysis of variance and the determination of confidence intervals, with the statistical package Statistical Analysis System, version 6.08 (SAS Institute Inc., Cary, NC). All data are presented as means and standard deviations, indicated as "mean ± SD". Differences were considered to be statistically significant when the *P* values were less than 0.05.

## 3. Results and discussion

*3.1. Preparation and characterization of nanoparticles*

Berberine/heparin nanoparticles were produced by the ionic gelation of positively charged berberine with negatively charged heparin. As shown in Table 1, berberine:heparin in distinct compositions (0.0375%:0.0083%, 0.0375%:0.0167%, 0.0375%:0.0333, 0.0375%:0.0500%, and 0.0375%:0.0667% by w/v) have a mean size range of 700–4000 nm, with negative zeta potentials, depending on the relative concentrations of berberine and heparin used (Table 1). The particles size distributions, polydispersity indices (PDI) and zeta potentials of the prepared nanoparticles of berberine:heparin at 0.0375%:0.0167% and 0.0375%:0.0500% (w/v) composition in aqueous solution are presented in Figure 2. As shown in Table 1 and Figure 2, the zeta potential value of berberine/heparin nanoparticles (berberine:heparin = 0.0375%:0.0500%) was significantly lower than that of berberine:heparin compositions at 0.0375%:0.0167%, due to the significantly higher amounts of the negatively charged heparin being exposed on their surfaces. Additionally, berberine:heparin compositions at 0.0375%:0.0500% had a smaller particle size (688.6 ± 21.9 nm) with a narrower distribution (PDI 0.51 ± 0.11) than their counterpart berberine:heparin = 0.0375%:0.0167% (Figure 2). Therefore, the berberine:heparin composition of 0.0375%:0.0500% was chosen for use throughout

the rest of the study.

Heparin (structure shown in Figure 1) is a polydispersed, highly sulfated polysaccharide composed of repeating 1→4 linked uronic acid and glucosamine residues. There are three types of acidic functional groups (sulfate monoesters, sulfamido groups and carboxylate groups) present in the heparin polymer [3]. Berberine (structure shown in Figure 1) is a yellow–colored quaternary protoberberine alkaloid extracted from the root of the *Berberis* species shrubs or the bark of the Amur cork tree [29,30]. When prepared in distilled water, berberine, like heparin, is ionized. When prepared in combination the ionized berberine and heparin can form polyelectrolyte complexes (berberine/heparin nanoparticles) by electrostatic interactions between the positively charged ($–CN^+$) on berberine and the negatively charged ($–SO_4^–$ and $–COO^–$) on heparin. In the Fourier transform infrared (FTIR) spectra (Figure 3), peaks occur at 1615 $cm^{–1}$ for the cyano cation ($–CN^+$) on berberine and at 1229 $cm^{–1}$ and 1635 $cm^{–1}$ for the sulfate ions ($–SO_4^–$) and carboxylic ions ($–COO^–$), respectively, on heparin [3,31]. As shown, berberine/heparin nanoparticles lose the cyano cation characteristic peak at 1615 $cm^{–1}$, but gain a new peak at 1619 $cm^{–1}$; in addition, the characteristic peak of sulfate and carboxylic ions on heparin at 1229 $cm^{–1}$ and 1635 $cm^{–1}$ shifted to 1235 $cm^{–1}$ and 1639 $cm^{–1}$. The ionized berberine and heparin were, therefore, able to form polyelectrolyte complexes *via* electrostatic interactions.

However, the results obtained by the TEM examination showed that the morphology of the prepared berberine/heparin nanoparticles was irregular and oval shaped (Figure 1). To improve the complex formed, chitosan was blended with the berberine/heparin complex (Figure 1). The cationic polysaccharide chitosan is derived from chitin by alkaline deacetylation [32]. In our nanoparticles which were prepared with different concentratios of chitosan (0.00%, 0.02%, 0.04%, and 0.08% by w/v), the size distribution and zeta potential in an aqueous environment were investigated by a dynamic light scattering analyzer. As shown in Table 2, as the amount of chitosan incorporated was increased, the size of the resulting nanoparticles decreased

appreciably; meanwhile, the zeta potential value increased noticeably as more chitosan was incorporated, with the exception of the chitosan concentration 0.08%. The polydispersity index of nanoparticles measured by a dynamic light scattering analyzer revealed a narrower distribution (PDI 0.39 ± 0.07) than those berberine/heparin nanoparticles not incorporating chitosan (Figure 2). The characteristic FT–IR spectrum peak at 1573 $cm^{-1}$ that corresponds to the protonated amino group ($–NH_3^+$) in aqueous chitosan (pH 6.0) was shifted to 1590 $cm^{-1}$ in the prepared berberine/heparin/chitosan nanoparticles (Figure 3). Meanwhile, the characteristic peak for the negatively charged ($–SO_4^–$ and $–COO^–$) on heparin was shifted and decreased. These observations can be attributed to the electrostatic interaction between the negatively charged groups on heparin and the positively charged group on chitosan.

The particulate system for translocation permeabilities through gastrointestinal mucin was found to be decreased as the particle size increased [33]. The PDI is a measure of dispersion homogeneity and ranges from 0 to 1. Values close to 0 indicate a homogeneous dispersion while those greater than 0.3 indicate high heterogeneity [34]. As shown in Table 3, the berberine-loaded nanoparticles were obtained instantaneously upon addition of a thoroughly mixed aqueous berberine/heparin to a chitosan solution under magnetic stirring at room temperature. Table 3 and Figure 2 show the particle size, zeta potential, loading efficiency and PDI of the obtained nanoparticles. In the loading process, increasing the amount of berberine led to a larger overall size of the nanoparticles and to a significant increase in their berberine loading efficiency. When the berberine concentration was 0.0250% (w/v), the particle size, loading efficiency and PDI of the nanoparticles was 256.5 ± 2.3 nm, 54.4 ± 3.4% and 0.26 ± 0.02, respectively. Under this specific condition, the berberine-loaded nanoparticles remained spherical (Figure 1). As the berberine concentration was increased, the nanoparticle size became larger, yielding a mean particle size of more than 300 nm. Therefore, the optimal berberine concentration of 0.0250% (w/v) was chosen for subsequent *in vitro* study.

*3.2. In vitro drug release*

The release profiles of berberine from nanoparticles were investigated in simulated dissolution medium (pH 1.2 for 120 min, pH 6.0 for 120 min, then pH 7.0 for 240 min, simulating gastric acid, gastric mucosa and the *H. pylori* survival situation), respectively. Figure 4a shows the release profiles of berberine from the prepared nanoparticles at pH 1.2, 6.0, and 7.0, respectively. Heparin is a polydispersed, highly sulfated polysaccharide composed of repeating 1→4–linked uronic acid and glucosamine residues. There are three types of acidic functional groups in the heparin polymer. The sulfate monoesters and sulfamido groups are both highly acidic, with pKa values ranging from 0.5 to 1.5, whereas the extra carboxylate groups are less acidic, with pKa values between 2 to 4 [3]. Chitosan is a weak base, and the amino group on chitosan has a pKa value of around 6.5 [3]. At pH 1.2 (simulating gastric acid), only some of the $–COO^-$ groups on heparin became protonated (–COOH), the amino groups ($–NH_3^+$) on chitosan and the acidic functional groups (sulfate ions; $–SO_4^–$) on heparin were ionized. Therefore, chitosan and heparin were able to form polyelectrolyte complexes via electrostatic interaction, but relatively weaker compared with that at prepared nanoparticle situation, resulting in the proportion of berberine released from the nanoparticles in 120 min was 18.98 ± 3.56% (Figure 4a). As shown, at pH 6.0 (simulating the environment of the gastric mucosa or the *H. pylori* survival situation), little of the $–NH_3^+$ groups on chitosan became deprotonated and the carboxylic ions ($–COO^-$) and sulfate ions ($–SO_4^–$) were ionized on heparin, this was followed by little release of berberine at pH 6.0, possibly due to the conjugation of berberine and heparin. At pH 7.0 (*H. pylori* survival situation), most of the $–NH_3^+$ groups on chitosan was deprotonated, the nanoparticles became unstable and broken apart, allowing rapid release of the berberine from the nanoparticles.

The HPLC method was developed and validated in order to quantify berberine. Satisfactory retention times and good resolution of berberine were achieved using reverse phase C18 columns and elution with acetonitrile–0.04 M $H_3PO_4$ (42:58; v/v) at a flow rate of 1.0 mL/min (Figure 4b, right). Berberine was quantified by ultraviolet

absorbance at 349 nm in the range of 1.0–8.0 mg/L ($R^2$ = 0.999). The linear regression equation for the calibration curve was y = 727528x+33975, where y represented the peak area ratio of berberine and x represented the concentration of berberine (mg/L). Comparative chromatographic studies revealed that berebrine released from nanoparticles with standard berberine solution yielded a pure peak at the same retention time of 6.96 min.

Berberine's chemical structure contains a quaternary protoberberine alkaloid and it is commercially available in various salt forms, such as berberine chloride and hemisulfate. ESI–MS experiments were employed to examine the properties of berberine release from nanoparticles in standard berberine solution (Figure 4b, left). Berberine exhibited a base peak at m/z = 336.2 for $M^+$ and all of the alkaloids displayed $[M\text{-}CH_3]^+$ = 321.4, $[M\text{-}2CH_3]^+$ = 306.5, $[M\text{-}C_2H_4O]^+$ = 292.5, and $[M\text{-}2CH_3\text{-}CO]^+$ = 278.4 as the base peaks, no matter what collision energy was used [35,36]. As evidenced by ESI–MS (Figure 4b), no significant conformational change was observed for the berberine released from nanoparticles, as compared to the standard berberine.

*3.3. In vitro growth inhibition study*

Berberine has been extensively used to treat gastroenteritis and diarrhea caused by bacteria since the 1950s when its clinical safety was experimentally confirmed [37]. Since then, berberine has been characterized as having multiple pharmacologic functions, including antibacterial, antiparasitic, antifungal, hypotensive, antitumoral, anti–inflammatory and inhibition of lymphocyte transformation [30,37]. Moreover, recent pharmacological studies have demonstrated that berberine can inhibit the arylamine *N-acetyltransferase* activity in strains of *H. pylori* collected from peptic ulcer patients [11]. *N*–acetyltransferase–catalyzed reactions are known to activate or detoxify arylamine carcinogens. A study on *H. pylori* demonstrated that berberine elicited a dose–dependent growth inhibition in the *H. pylori* cultures, and inhibited the growth of the *H. pylori* strains with a minimum inhibitory concentration (MIC) range

of 0.78 to 25.00 mg/L [12]. Figure 5 shows the percentage of *H. pylori* growth inhibition effected by treatment with various berberine concentrations (0.0, 3.0, 6.0, 12.0 by mg/L) for 24 hr. The evident growth inhibition observed at 6.0 mg/L was found to be 24.5 ± 3.3 (only berberine solution) and 35.3 ± 3.7 (berberine/heparin/chitosan nanoparticles). Berberine concentration of 12.0 mg/L was 42.4 ± 3.2 (only berberine solution) and 53.2 ± 2.9 (berberine/heparin/chitosan nanoparticles), compared to control (without sample). Our prepared berberine/heparin/chitosan nanoparticles with a negative surface charge (where heparin dominated the surface, berberine:heparin:chitosan = 0.0250%:0.0500%:0.0400% by w/v) were able to increase the values of *H. pylori* growth inhibition significantly ($p < 0.05$), compared to berberine solution. Heparin is found primarily in the liver, lungs and gut tissues, while its structural relative, heparin sulfate, resides in the extracellular cell matrix at the surface of most animal cells [38]. Heparin is normally produced by mast cells and is stored in intracellular granules until needed. Recent studies indicate that vacuolating cytotoxin A (VacA) is able to recruit and activate mast cells [39]. Moreover, the C-terminal domain of the 58 kDa subunit of *H. pylori* VacA can bind both heparin and heparan sulfate [40]. Therefore, when the negatively charged nanoparticles (berberine/heparin/chitosan) specifically interact with *H. pylori*, the drug is likely released from the nanoparticle to act locally.

### *3.4. cytotoxicity of berberine solution and berberine/heparin/chitosan nanoparticles*

The anti–neoplastic effects of berberine have drawn extensive attention of researchers hoping to exploit its therapeutic properties. Berberine has since been shown to suppress the growth of a wide variety of tumor cells, including breast cancer, epidermoid carcinoma, oral carcinoma, prostate carcinoma, and gastric carcinoma [41–43]. Lin *et al.* sought to determine the molecular mechanism of berberine that underlies its effects in human gastric cancer cells. Berberine (8.4–672.4 mg/L) was found to be cytotoxic to human gastric cancer cells in a dose-dependent manner, at an $IC_{50}$ of 16.1 mg/L [13]. In our study, the cytotoxicity of berberine solution and

berberine/neparin/chitosan nanoparticles were evaluated using human gastric adenocarcinoma cells by using an MTT assay (Figure 6). The reduction of cell viability after treatment was significantly higher with 12 mg/L of berberine for all test samples. Cell viability was generally not affected by 3.0 and 6.0 mg/L of berberine. To examine the relationship between *H. pylori* and the prepared berberine/heparin/chitosan nanoparticles without damaging the cultured cells, test samples were prepared at a constant berberine concentration of 6.0 mg/L throughout the rest of the study.

*3.5. Association of fluorescent H. pylori and nanoparticles with AGS cells*

To observe the adhesion capabilities of *H. pylori* to the human gastric mucosal AGS cells, the bacterium was fluorescently labeled with DilC18(5)–DS lipophilic dye to form the DilC18(5)–labeled *H. pylori*. As shown in Figure 7, after 2 hr of infection, the AGS-adapted DilC18(5)–*H. pylori* (magenta; yellow arrows) preferentially targeted cell–cell junctions and was observed within the cells. It was confirmed that *H. pylori* strains mainly resided in the gastric mucosa or at the interface with the mucus layer, and produced the vacuolating cytotoxin, which modulates the integrity of the tight junctions of the epithelium and reduces the stability of the cytoskeleton. In order to examine the allocation of negative surface charge (heparin dominated on the surface) nanoparticles in the AGS cell after 2 hr exposure, fluorescent nanoparticles (berberine/FA–heparin/chitosan nanoparticles) were used. Heparin is a member of the glycosaminoglycan family of carbohydrates (which includes the closely related molecule heparan sulfate) and consists of a variably sulfated repeating disaccharide unit. Among which heparan sulfate is a ubiquitously expressed heparin analog that appears as a proteoglycan at the cell surface [17,37]. The distribution of berberine (blue) and FA-heparin (green) in the intercellular spaces was observed by CLSM. The natural yellow color of berberine has made it useful as a commercial dye; its normal excitation occurs at about 350 nm with UV laser system [26,44]. The synthesis of FA–heparin was based on the reaction between the amine groups of FA and the

carboxylic acid groups of heparin; FA excitation occurs at 488 nm using an argon laser. As shown in Figure 7, after 2 hr of incubation of berberine/FA–heparin/chitosan nanoparticles the incubated nanoparticles were located in the same intercellular spaces and cell cytoplasm (as indicated by superimposed green/blue spots; i.e., white arrows) when internalized into the cytoplasm.

*3.6. Evaluating the relationship between H. pylori and nanoparticles*

Figure 8a shows the influence of *H. pylori* infection alone or after pretreatment with berberine/heparin/chitosna nanoparticles on gastric mucosal cell viability. Significant inhibition of AGS cell viability after infection with only *H. pylori* ($8 \times 10^8$ CFU/mL) was observed to be 51.6 ± 6.2%, as compared to uninfected controls. *H. pylori* colonization of the gastric mucosa is associated with alterations in gastric epithelial cell cycle events, a condition implicated in the initiation and development of gastric cancer. Virulence factors of *H. pylori* include urease, lipopolysaccharides, adhesins, the cytotoxin–associated gene A product and have been determined to contribute to host inflammation and epithelial cell damage, such as cytoplasmic vacuolation and induction of apoptosis [45]. In our study, the berberine/heparin/chitosna nanoparticles with berberine concentration 3.0 and 6.0 mg/L caused a statistically significant increase in AGS cell growth. Cell growth was enhanced in a dose-dependent manner, as shown in Figure 8a; specifically, in *H. pylori* infected cells, berberine stimulated an almost 1.3-fold cell growth increase at a dose of 3.0 mg/L and a 1.6-fold growth increase at a dose of 6.0 mg/L. Therefore, berberine/heparin/chitosan nanoparticles were able to efficiently reduce the cytotoxic effects of *H. pylori* in AGS cells.

The *in situ* adherence assay was carried out by using fluorescently labeled DilC18(5)–*H. pylori* that had been incubated with berberine/FA-heparin/chitosan nanopaticles (berberine concentration at 6.0 mg/L) (Figure 8b). As can be seen, the AGS-adapted DilC18(5)–*H. pylori* (magenta) preferentially targeted cell–cell junctions and were located within the cells. AGS cells were then incubated with

fluorescent berberine/FA–heparin/chitosan nanoparticles (FA–heparin; green spots and berberine; blue spots) to ascertain whether the nanoparticles were attached in the same way to the intercellular spaces at the sites of *H. pylori* infection (white spot). The white spots in the superimposed images were observed to disappear, indicating the release of berberine from nanoparticles into the intercellular spaces or the cell cytoplasm (blue spots). From these results, we concluded that the nanoparticle drug delivery system could effectively release the berberine from the nanoparticle so that it may act locally on *H. pylori* at an appropriate bactericidal concentration.

## 4. Conclusions

We developed a novel nanoparticle carrier shelled with heparin for berberine delivery to treat *H. pylori.* The *in vitro* analysis of drug release from the nanoparticle indicated that the system is able to control berberine release in the simulated gastrointestinal dissolution medium, and that the berberine was able to localize specifically to intercellular spaces or in the cell cytoplasm, the site of *H. pylori* infection. Furthermore, the prepared berberine/heparin/chitosan nanoparticles were able to increase the values of *H. pylori* growth inhibition significantly, compared to berberine alone in solution, and to efficiently decrease the cytotoxic effects of *H. pylori* infection of the cells.

## Acknowledgements

This work was supported by grants from the National Science Council (NSC 98-2815-C-039-034-B) and the Center for Inflammation Research, China Medical University (CMU 98-N1-08 and CMU 98-CT-12), Republic of China. The confocal microscopy SP2 experiment and Zetasizer apparatus supported by the Medical Research Core Facilities center, Office of Research & Development, China Medical University were gratefully acknowledged.

## References


[1] Goodman KJ, Cockburn M. The role of epidemiology in understanding the health effects of Helicobacter pylori. Epidemiology 2001;12:266–271.

[2] Beil W, Kilian P. EPs 7630, an extract from Pelargonium sidoides roots inhibits adherence of Helicobacter pylori to gastric epithelial cells. Phytomedicine 2007; 14:5–8.

[3] Lin YH, Chang CH, Wu YS, Hsu YM, Chiou SF, Chen YJ. Development of pH-responsive chitosan/heparin nanoparticles for stomach-specific anti-Helicobacter pylori therapy. Biomaterials 2009;30:3332–3342.

[4] Chang CH, Lin YH, Yeh CL, Chen YC, Chiou SF, Hsu YM, Chen YS, Wang CC. Nanoparticles incorporated in pH-sensitive hydrogels as amoxicillin delivery for eradication of Helicobacter pylori. Biomacromolecules 2010;11:133–142.

[5] Bardonnet PL, Faivre V, Pugh WJ, Piffaretti JC, Falson F. Gastroretentive dosage forms: overview and special case of Helicobacter pylori. J Controlled Release 2006;111:1–18.

[6] de Bortoli N, Leonardi G, Ciancia E, Merlo A, Bellini M, Costa F, Mumolo MG, Ricchiuti A, Cristiani F, Santi S, Rossi M, Marchi S. Helicobacter pylori eradication: A randomized prospective study of triple therapy versus triple therapy plus lactoferrin and probiotics. Am J Gastroenterol 2007;102:951–956.

[7] Li Y, Xu C, Zhang Q, Liu JY, Tan RX. In vitro anti–Helicobacter pylori action of 30 Chinese herbal medicines used to treat ulcer diseases. J Ethnopharmacol 2005; 98:329–333.

[8] Wang F, Zhou HY, Zhao G, Fu LY, Cheng L, Chen JG, Yao WX. Inhibitory effects of berberine on ion channels of rat hepatocytes. World J Gastroenterol 2004;10: 2842–2845.

[9] Baird AW, Taylor CT, Brayden DJ. Non-antibiotic anti-diarrhoeal drugs: factors affecting oral bioavailability of berberine and loperamide in intestinal tissue. Adv Drug Deliv Rev 1997;23:111–120.

[10] Chung JG, Wu LT, Chang SH, Lo HH, Hsieh SE, Li YC, Hung CF. Inhibitory actions of berberine on growth and arylamine N-acetyltransferase activity in strains of helicobacter pylori from peptic ulcer patients. Int J Toxicol 1999;18: 35–40.

[11] Mahady GB, Pendland SL, Stoia A, Chadwick LR. In vitro susceptibility of Helicobacter pylori to isoquinoline alkaloids from Sanguinaria canadensis and Hydrastis canadensis. Phytother Res 2003;17:217–221.

[12] Lin JP, Yang JS, Lee JH, Hsieh WT, Chung JG. Berberine induces cell cycle arrest and apoptosis in human gastric carcinoma SNU-5 cell line. World J

Gastroenterol 2006;12:21–28.

[13] Pan LR, Tang Q, Fu Q, Hu BR, Xiang JZ, Qian JQ. Roles of nitric oxide in protective effect of berberine in ethanol-induced gastric ulcer mice. Acta Pharmacol Sin 2005;26:1334–1338.

[14] Bentolila A, Vlodavsky I, Haloun C, Domb AJ. Synthesis and heparin-like biological activity of amino acid-based polymers. Polym Adv Technol 2000;11: 377–387.

[15] Bertolesi G, Eijan AM, Calvo JC, Lauria de Cidre L. Heparin increases the adhesion of murine mammary adenocarcinoma cells (LM3). Correlation with the presence of heparin receptors on cell surface. J Biol Regul Homeost Agents 2005; 19:33–40.

[16] Benoit DS, Anseth KS. Heparin functionalized PEG gels that modulate protein adsorption for hMSC adhesion and differentiation. Acta Biomater 2005;1:461–470.

[17] Thein-Han WW, Misra RD. Acta Biomater. Biomimetic chitosan-nanohydroxyapatite composite scaffolds for bone tissue engineering. Acta Biomater 2009;5:1182–1197.

[18] van der Lubben IM, Verhoef JC, Borchard G, Junginger HE. Chitosan and its derivatives in mucosal drug and vaccine delivery. Eur J Pharm Sci 2001;14: 201–207.

[19] Erbacher P, Zou S, Bettinger T, Steffan AM, Remy JS. Chitosan-based vector/DNA complexes for gene delivery: biophysical characteristics and transfection ability. Pharm Res 1998;15:1332–1339.

[20] Hall AJ, Tripp M, Howell T, Darland G, Bland JS, Babish JG. Gastric mucosal cell model for estimating relative gastrointestinal toxicity of non-steroidal anti-inflammatory drugs. Prostaglandins Leukot Essent Fatty Acids 2006;75:9–17.

[21] Kuno T, Naito S, Ohta M, Kido N, Ito H, Kato N. Staining of O-specific polysaccharide chains of lipopolysaccharides with ruthenium red. Microbiol Immunol 1986;30:743–751.

[22] Wang SD, Song BS, Li K. Determination of berberine in decocted liquid from shenshu granules with water by reversed-phase liquid chromatography. Se Pu 2000;18:261–262.

[23] Sahasathian T, Kerdcholpetch T, Chanweroch A, Praphairaksit N, Suwonjandee N, Muangsin N. Sustained release of amoxilcilline from chitosan tablets. Arch

Pharm Res 2007;30:526–531.

[24] Pan JF, Yu C, Zhu DY, Zhang H, Zeng JF, Jiang SH, Ren JY. Identification of three sulfate–conjugated metabolites of berberine chloride in healthy volunteers' urine after oral administration. Acta Pharmacol Sin 2002;23:77–82.

[25] Jain P, Jain S, Prasad KN, Jain SK, Vyas SP. Polyelectrolyte coated multilayered liposomes (nanoparticles) for the treatment of Helicobacter pylori infection. Mol. Pharm. 2009, 6, 593–603.

[26] Sakai T, Ohno N, Chung YS, Nishikawa H. Spectrofluorimetric determination of berberine in oriental pharmaceutical preparations by flow-injection analysis coupled with liquid-liquid extraction. Anal Chim Acta 1995;308:329–333.

[27] Sieveking D, Leach ST, Mitchell HM, Day AS. Role of serum factors in epithelial cell responses to Helicobacter pylori infection in vitro. J Gastroenterol Hepatol 2005;20:1610–1615.

[28] Lai CH, Fang SH, Rao YK, Geethangili M, Tang CH, Lin YJ, Hung CH, Wang WC, Tzeng YM. Inhibition of Helicobacter pylori-induced inflammation in human gastric epithelial AGS cells by Phyllanthus urinaria extracts. J Ethnopharmacol 2008;118;522–526.

[29] Hsieh YS, Kuo WH, Lin TW, Chang HR, Lin TH, Chen PN, Chu SC. Protective effects of berberine against low-density lipoprotein (LDL) oxidation and oxidized LDL-induced cytotoxicity on endothelial cells. J Agric Food Chem 2007;55: 10437–10445.

[30] Li Y, He WY, Tian J, Tang J, Hu Z, Chen X. The effect of Berberine on the secondary structure of human serum albumin. J Mol Struct 2005;743;79–84.

[31] Kim Y, Kim SJ, Nam W. A ferric-cyanide-bridged one-dimensional dirhodium complex with (18–crown–6)potassium cations. Acta Crystallogr C 2001;57: 266–268.

[32] Lin YH, Chung CK, Chen CT, Liang HF, Chen SC, Sung HW. Preparation of nanoparticles composed of chitosan/poly-γ-glutamic acid and evaluation of their permeability through caco-2 cells. Biomacromolecules 2005;6:1104–1112.

[33] Norris DA, Sinko PJ. Effect of size, surface charge, and hydrophobicity on the translocation of polystyrene microspheres through gastrointestinal mucin. J Appl Polym Sci 1998;63;1481–1492.

[34] Ahlin P, Kristl J, Kristl A, Vrecer F. Investigation of polymeric nanoparticles as carriers of enalaprilat for oral administration. Int J Pharm 2002;239:113–120.

[35] Wu W, Song F, Yan C, Liu Z, Liu S. Structural analyses of protoberberine alkaloids in medicine herbs by using ESI-FT-ICR-MS and HPLC-ESI-MS(n). J Pharm Biomed Anal 2005;37;437–446.

[36] Chen YR, Wen KC, Her GR. Analysis of coptisine, berberine and palmatine in

adulterated Chinese medicine by capillary electrophoresis-electrospray ion trap mass spectrometry. J Chromatogr A 2000;866:273–280.

[37] Yang P, Song DQ, Li YH, Kong WJ, Wang YX, Gao LM, Liu SY, Cao RQ, Jiang JD. Synthesis and structure–activity relationships of berberine analogues as a novel class of low-density-lipoprotein receptor up-regulators. Bioorg Med Chem Lett 2008;18:4675–4677.

[38] Dubreuil JD, Ruggiero P, Rappuoli R, Del Giudice G. Effect of heparin binding on Helicobacter pylori resistance to serum. J Med Microbiol 2004;53:9–12.

[39] Supajatura V, Ushio H, Wada A, Yahiro K, Okumura K, Ogawa H, Hirayama T, Ra C. VacA, a vacuolating cytotoxin of Helicobacter pylori, directly activates mast cells for migration and production of proinflammatory cytokines. J Immunol 2002; 168:2603–2607.

[40] Utt M, Danielsson B, Wadström T. Helicobacter pylori vacuolating cytotoxin binding to a putative cell surface receptor, heparan sulfate, studied by surface plasmon resonance. FEMS Immunol Med Microbiol 2001;30:109–113.

[41] Kim JB, Yu JH, Ko E, Lee KW, Song AK, Park SY, Shin I, Han W, Noh DY. The alkaloid Berberine inhibits the growth of Anoikis-resistant MCF-7 and MDA-MB-231 breast cancer cell lines by inducing cell cycle arrest. Phytomedicine 2010;17:436–440.

[42] Ho YT, Lu CC, Yang JS, Chiang JH, Li TC, Ip SW, Hsia TC, Liao CL, Lin JG, Wood WG, Chung JG. Berberine induced apoptosis via promoting the expression of caspase-8, -9 and -3, apoptosis-inducing factor and endonuclease G in SCC-4 human tongue squamous carcinoma cancer cells. Anticancer Res 2009;29: 4063–4070.

[43] Auyeung KK, Ko JK. Coptis chinensis inhibits hepatocellular carcinoma cell growth through nonsteroidal anti–inflammatory drug-activated gene activation. Int J Mol Med 2009;24:571–577.

[44] Pereira CV, Machado NG, Oliveira PJ. Mechanisms of berberine (natural yellow 18)–induced mitochondrial dysfunction: interaction with the adenine nucleotide translocator. Toxicol Sci 2008;105:408–417.

[45] Kuck D, Kolmerer B, Iking-Konert C, Krammer PH, Stremmel W, Rudi J. Vacuolating cytotoxin of Helicobacter pylori induces apoptosisin the human gastric epithelial cell line AGS. Infect Immun 2001;69:5080–5087.

**Tables**

Table 1. Particle sizes and zeta potentials of nanoparticles prepared with different concentration berberine/heparin in deionized water (n = 5).

| Berberine Concentration (w/v) | Heparin Concentration (w/v) | Mean Particle Size (nm) | Zeta Potential (mV) |
|---|---|---|---|
| 0.0375% | 0.0083% | 4103.8 ± 587.6 | -27.2 ± 0.9 |
| 0.0375% | 0.0167% | 1958.2 ± 185.1 | -32.6 ± 2.3 |
| 0.0375% | 0.0333% | 981.9 ± 59.7 | -47.3 ± 3.1 |
| 0.0375% | 0.0500% | 688.6 ± 21.9 | -59.0 ± 0.6 |
| 0.0375% | 0.0667% | 701.9 ± 17.5 | -60.1 ± 1.7 |

Table 2. Effect of different concentration chitosan on particle sizes and zeta potential values of the berberine/heparin/chitosan nanoparticles (n = 5).

| Berberine/Heparin Concentration (w/v) | 0.0375%/0.0500% | |
|---|---|---|
| **Chitosan Concentration (w/v)** | **Mean Particle Size (nm)** | **Zeta Potential (mV)** |
| 0.00% | 688.6 ± 21.9 | -59.0 ± 0.6 |
| 0.02% | 590.7 ± 22.5 | -51.7 ± 1.1 |
| 0.04% | 403.8 ± 8.9 | -44.8 ± 0.6 |
| 0.08% | ■ | ■ |

■ Precipitation of aggregates was observed.

Table 3. Effect of different concentration berine on particle sizes and zeta potential values of the berberine/heparin/chitosan nanoparticles (n = 5).

| Heparin/Chitosan Concentration (w/v) | 0.05%/0.04% | | |
|---|---|---|---|
| **Berberine Concentration (w/v)** | **Mean Particle Size (nm)** | **Zeta Potential (mV)** | **Loading Efficiency (%)** |
| 0.0200% | 225.7 ± 2.9 | -46.9 ± 0.1 | 27.4 ± 2.5 |
| 0.0250% | 256.5 ± 2.3 | -46.1 ± 0.4 | 54.4 ± 3.4 |
| 0.0300% | 321.9 ± 9.7 | -44.5 ± 0.2 | 64.4 ± 4.6 |
| 0.0375% | 403.8 ± 8.9 | -43.8 ± 0.6 | 79.1 ± 6.5 |

**Figure Captions**

Fig. 1. Schematic illustrations of the internal structures and TEM micrographs of berberine/heparin nanoparticles and berberine/heparin/chitosan nanoparticles.

Fig. 2. Particle size distribution and zeta potential of the prepared nanoparticles (berberine/heparin nanoparticles and berberine/heparin/chitosan nanoparticles) at distinct compositions.

Fig. 3. FT–IR spectra of heparin, berberine, chitosan, berberine/heparin nanoparticles and berberine/heparin/chitosan nanoparticles.

Fig. 4. (a) *In vitro* release profiles of berberine from nanoparticles at different pH values at 37℃ (n =5). (b) HPLC and ESI–MS spectra of standard berberine and berberine released from nanoparticles. HPLC: high–performance liquid chromatography; ESI–MS: electrospray ionization–mass spectrometer.

Fig. 5. Percentage of *H. Pylori* growth inhibition of only berberine solution and berberine/heparin/chitosan nanoparticles.

Fig. 6. Cell viability after treatment with only berberine solution and berberine/heparin/chitosna nanoparticles after distince berberine concentration, determined by MTT assay (n = 6). MTT: 3-(4,5-dimethyl-thiazol-yl)-2,5-diphenyltetrazolium bromide.

Fig. 7. Confocal images of AGS cells infected with *H. pylori* or with internalized berberine/FA–heparin/chitosan nanoparticles for 2 hr. AGS cells: human gastric adenocarcinoma cells; FA: fluoresceinamine isomer I.

Fig. 8. (a) Changes in cell growth after *H. pylori* infection and berberine/FA–heparin/chitosan nanoparticles pretreatment. AGS cells were preincubated for 2 hr with test nanoparticles and then infected with *H. pyloi* respectively. (b) Fluorescent images (taken with confocal laser scanning microscope) of cells infected with *H. pylori* and incubated with berberine/FA–heparin/chitosan nanoparticles. AGS cells: human gastric adenocarcinoma cells; FA: fluoresceinamine isomer I.

Figure(s)

# Figure 1

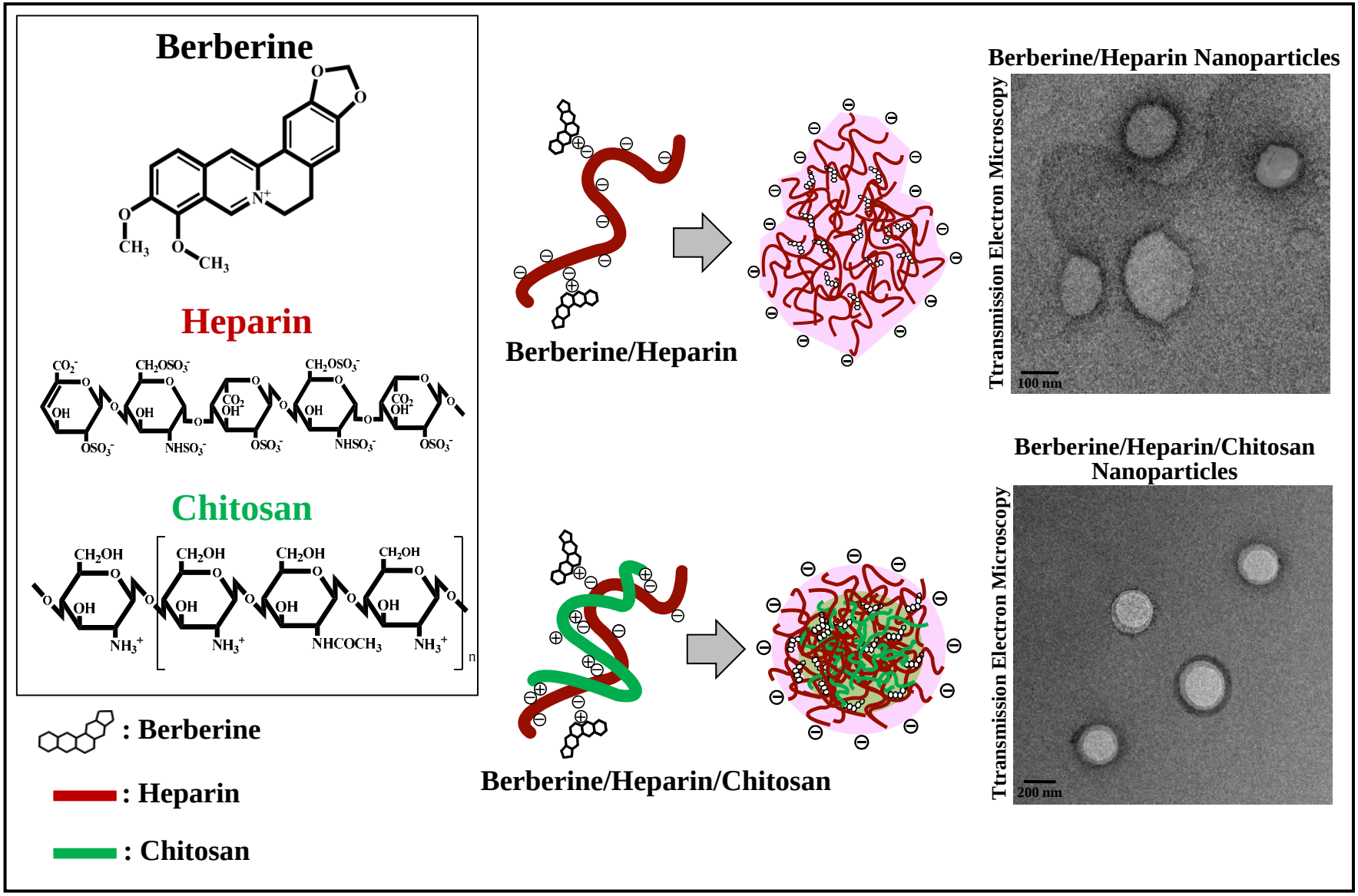

# Figure 2

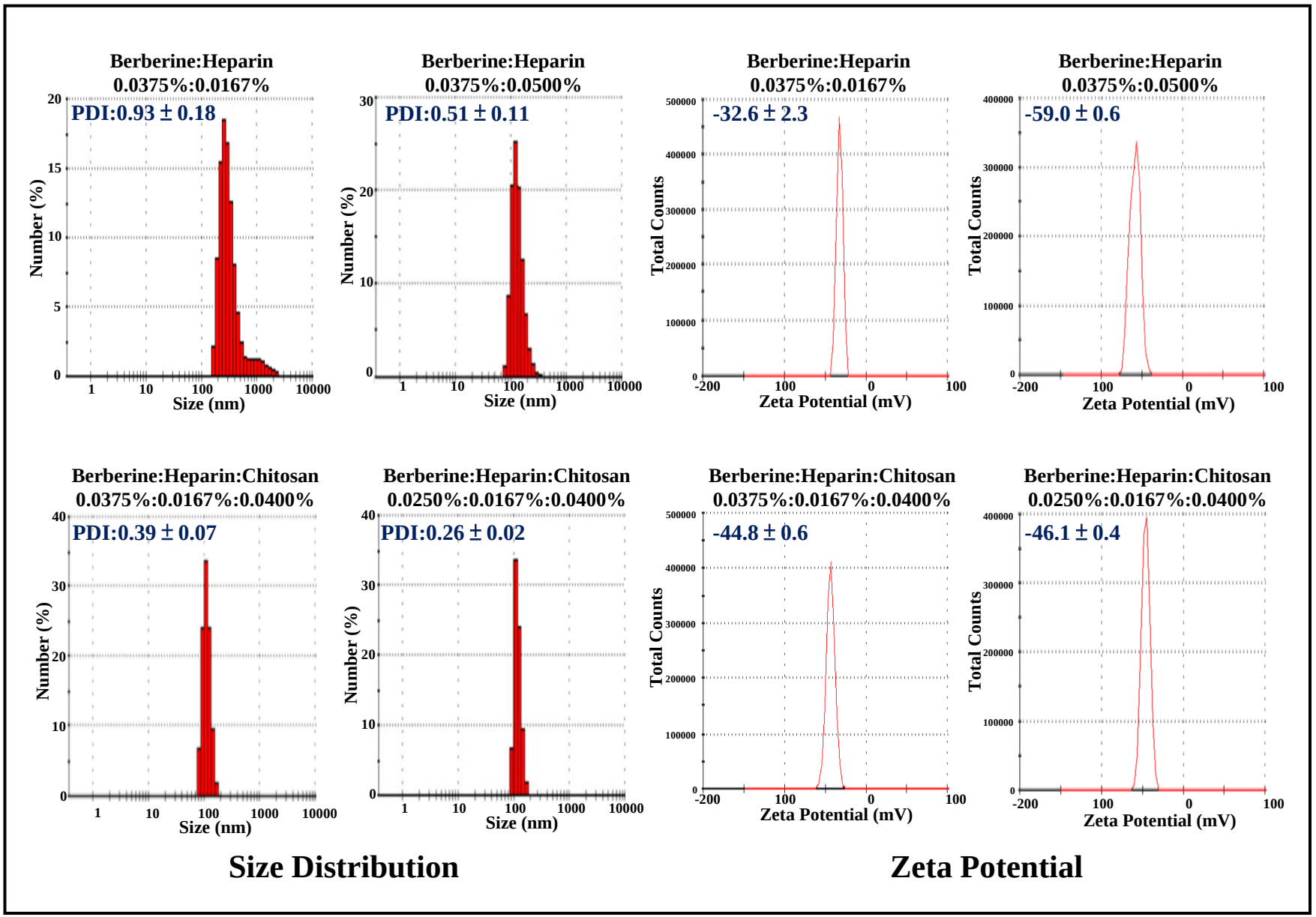
Berberine:Heparin
0.0375%:0.0167%
PDI:0.93 ± 0.18
Number (%)
Size (nm)
Berberine:Heparin
0.0375%:0.0500%
PDI:0.51 ± 0.11
Number (%)
Size (nm)
Berberine:Heparin
0.0375%:0.0167%
-32.6 ± 2.3
Total Counts
Zeta Potential (mV)
Berberine:Heparin
0.0375%:0.0500%
-59.0 ± 0.6
Total Counts
Zeta Potential (mV)
Berberine:Heparin:Chitosan
0.0375%:0.0167%:0.0400%
PDI:0.39 ± 0.07
Number (%)
Size (nm)
Berberine:Heparin:Chitosan
0.0250%:0.0167%:0.0400%
PDI:0.26 ± 0.02
Number (%)
Size (nm)
Berberine:Heparin:Chitosan
0.0375%:0.0167%:0.0400%
-44.8 ± 0.6
Total Counts
Zeta Potential (mV)
Berberine:Heparin:Chitosan
0.0250%:0.0167%:0.0400%
-46.1 ± 0.4
Total Counts
Zeta Potential (mV)
Size Distribution
Zeta Potential

**Figure 3**

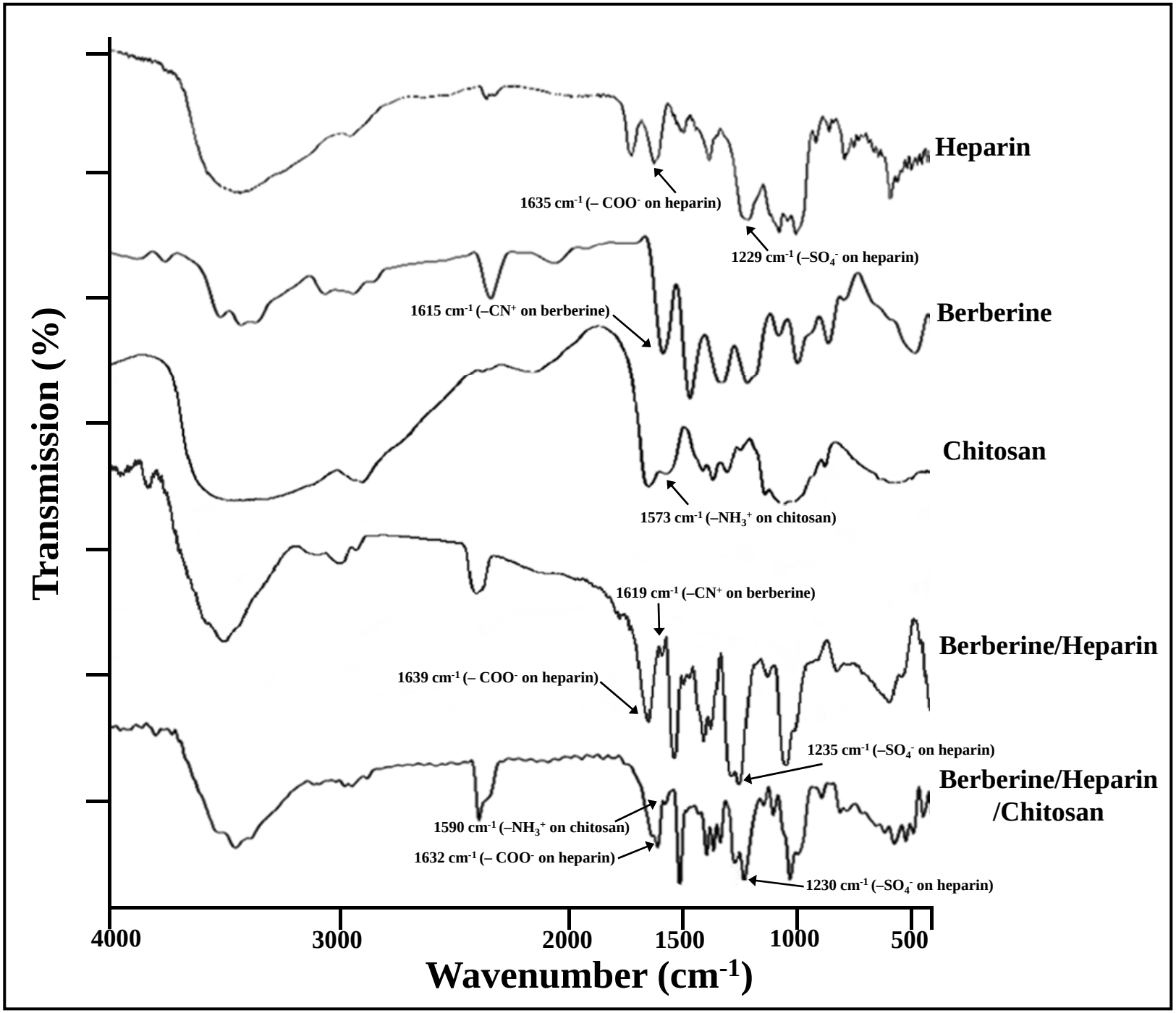
Transmission (%)
Heparin
1635 cm-1 (– COO- on heparin)
1229 cm-1 (–SO4- on heparin)
Berberine
1615 cm-1 (–CN+ on berberine)
Chitosan
1573 cm-1 (–NH3+ on chitosan)
Berberine/Heparin
1619 cm-1 (–CN+ on berberine)
1639 cm-1 (– COO- on heparin)
1235 cm-1 (–SO4- on heparin)
Berberine/Heparin /Chitosan
1590 cm-1 (–NH3+ on chitosan)
1632 cm-1 (– COO- on heparin)
1230 cm-1 (–SO4- on heparin)
4000
3000
2000
1500
1000
500
Wavenumber (cm-1)

**Figure 4a**

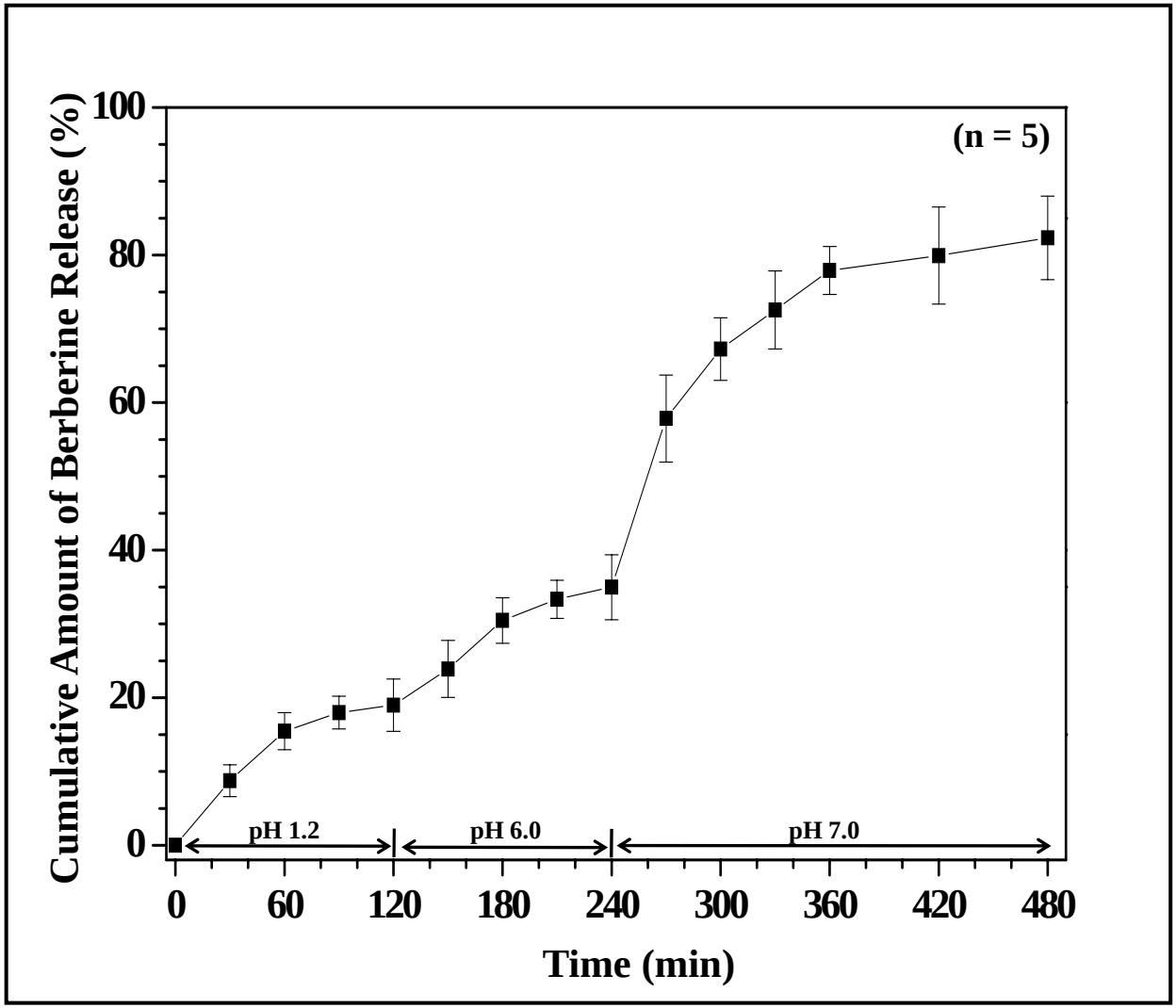
Cumulative Amount of Berberine Release (%)
100
80
60
40
20
0
(n = 5)
pH 1.2
pH 6.0
pH 7.0
0
60
120
180
240
300
360
420
480
Time (min)

# Figure 4b

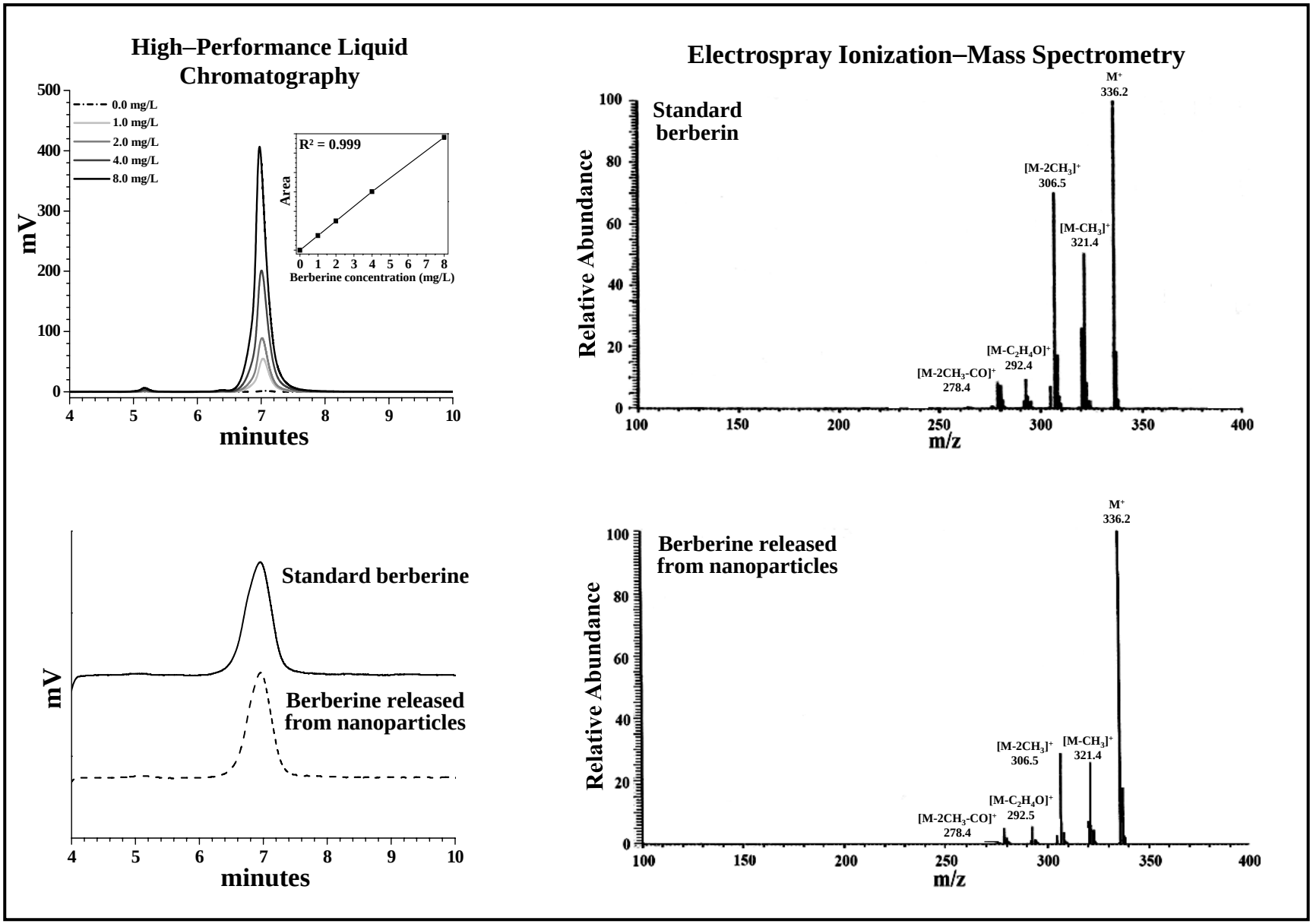
High–Performance Liquid Chromatography
0.0 mg/L
1.0 mg/L
2.0 mg/L
4.0 mg/L
8.0 mg/L
mV
minutes
R² = 0.999
Area
Berberine concentration (mg/L)
Standard berberine
Berberine released from nanoparticles
Electrospray Ionization–Mass Spectrometry
Standard berberin
Relative Abundance
m/z
M⁺ 336.2
[M-2CH3]⁺ 306.5
[M-CH3]⁺ 321.4
[M-C2H4O]⁺ 292.4
[M-2CH3-CO]⁺ 278.4
Berberine released from nanoparticles
M⁺ 336.2
[M-2CH3]⁺ 306.5
[M-CH3]⁺ 321.4
[M-C2H4O]⁺ 292.5
[M-2CH3-CO]⁺ 278.4

**Figure 5**

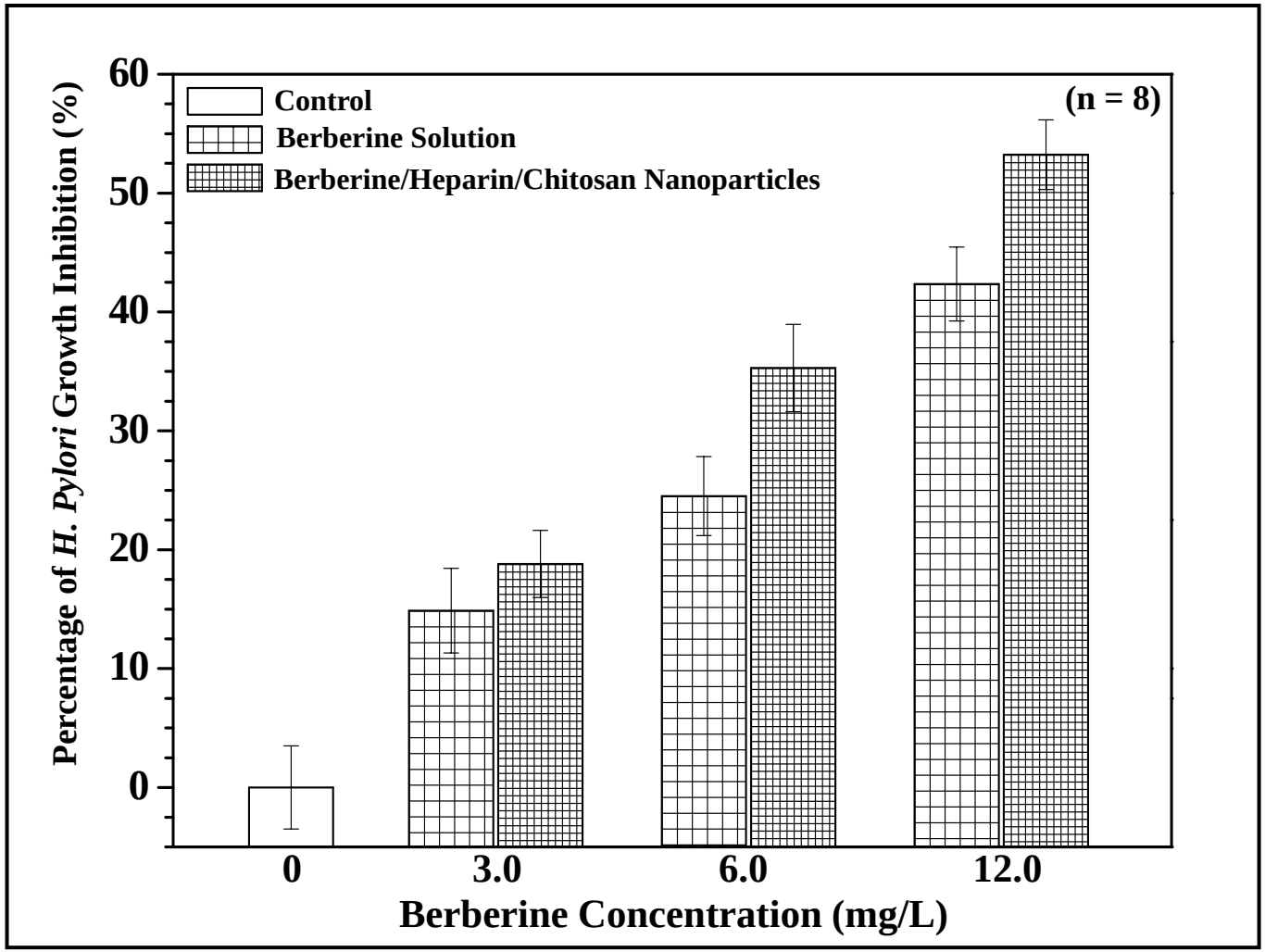
Control
Berberine Solution
Berberine/Heparin/Chitosan Nanoparticles
(n = 8)
Percentage of H. Pylori Growth Inhibition (%)
60
50
40
30
20
10
0
0
3.0
6.0
12.0
Berberine Concentration (mg/L)

**Figure 6**

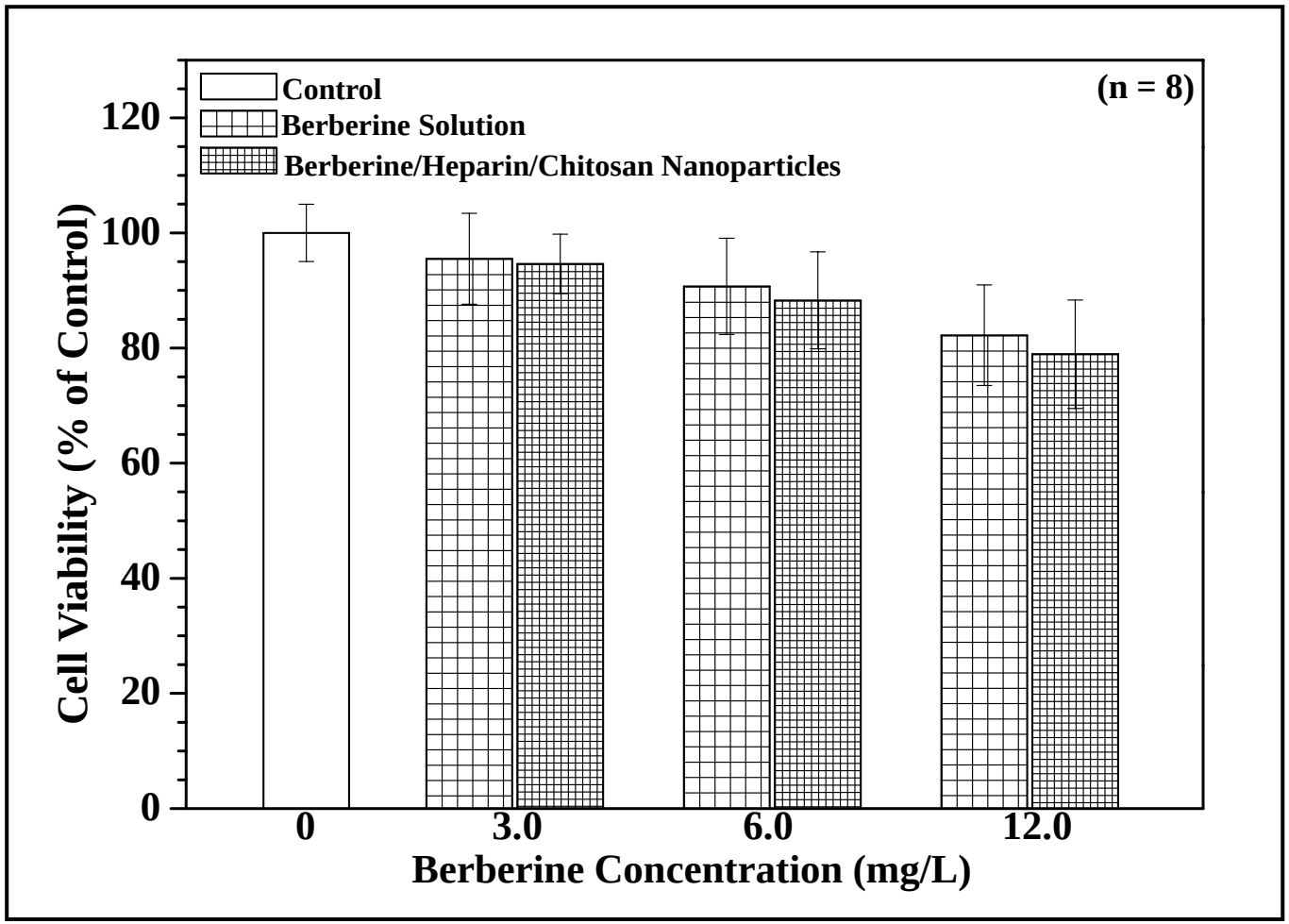
Control
Berberine Solution
Berberine/Heparin/Chitosan Nanoparticles
(n = 8)
Cell Viability (% of Control)
120
100
80
60
40
20
0
0
3.0
6.0
12.0
Berberine Concentration (mg/L)

**Figure 7**

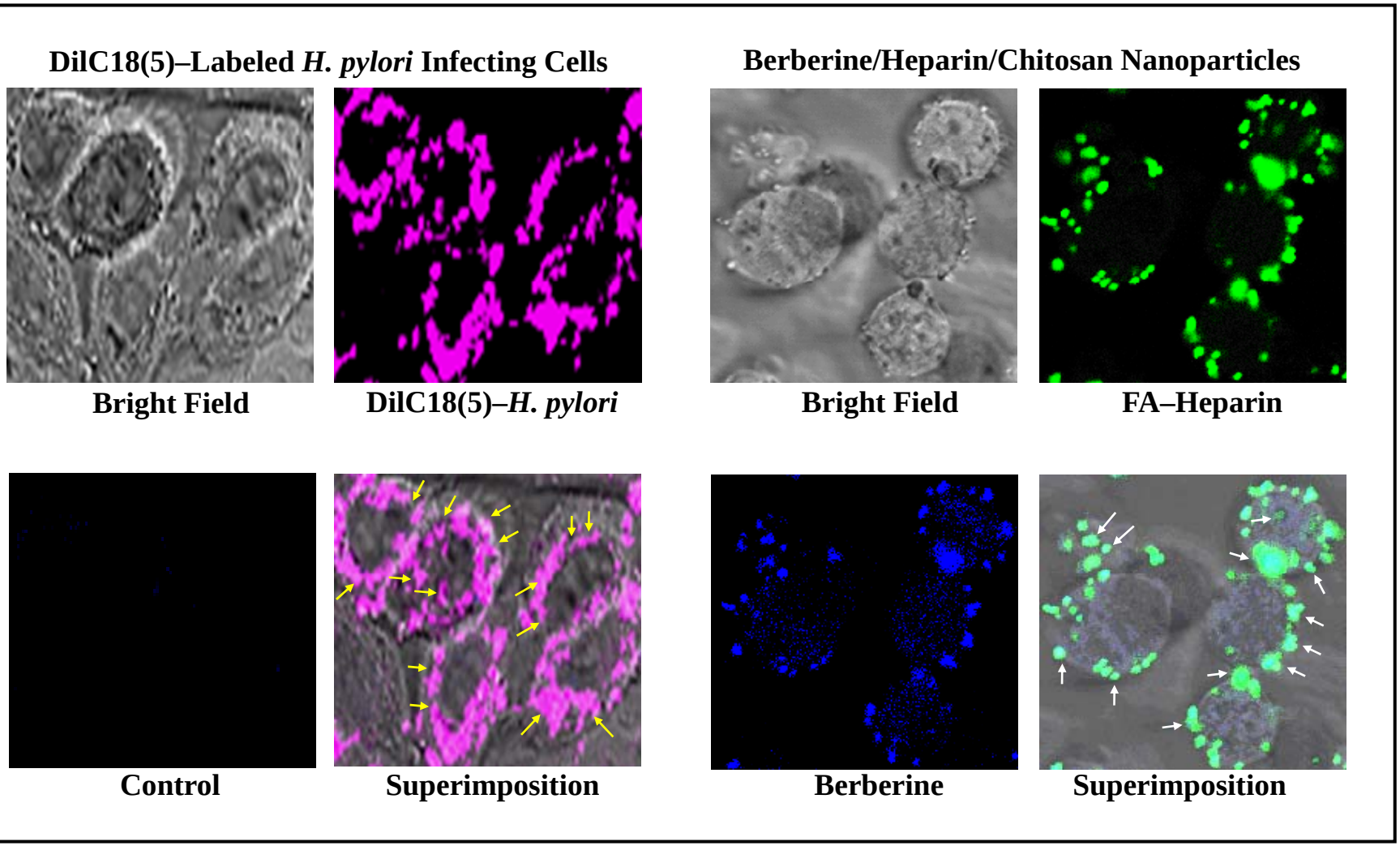
DilC18(5)–Labeled *H. pylori* Infecting Cells
Berberine/Heparin/Chitosan Nanoparticles
Bright Field
DilC18(5)–*H. pylori*
Bright Field
FA–Heparin
Control
Superimposition
Berberine
Superimposition

**Figure 8**

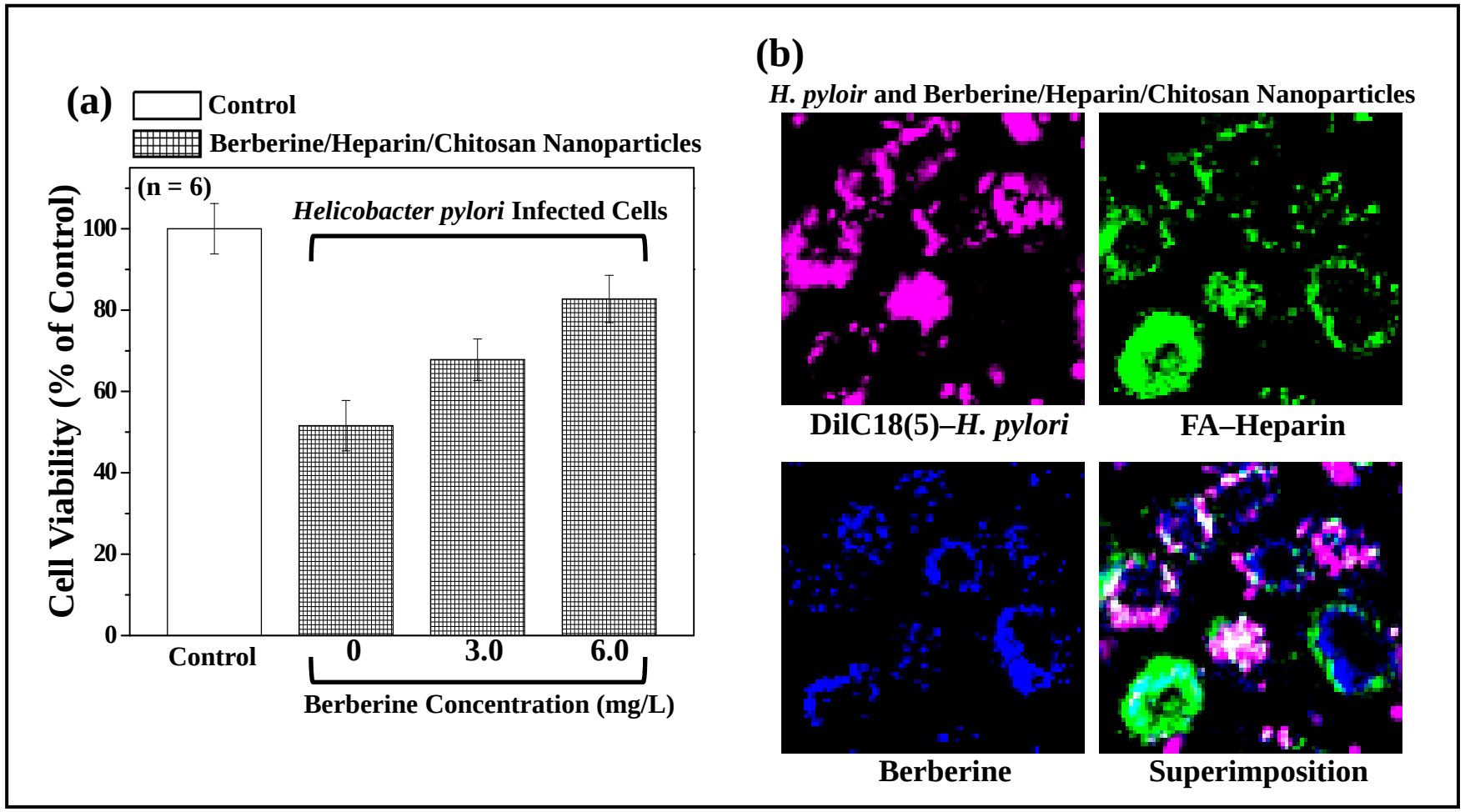
(a)
Control
Berberine/Heparin/Chitosan Nanoparticles
(n = 6)
Helicobacter pylori Infected Cells
Cell Viability (% of Control)
100
80
60
40
20
0
Control
0
3.0
6.0
Berberine Concentration (mg/L)
(b)
H. pyloir and Berberine/Heparin/Chitosan Nanoparticles
DilC18(5)–H. pylori
FA–Heparin
Berberine
Superimposition